

Population synthesis of young isolated neutron stars: the effect of fallback disk accretion and magnetic field evolution

Lei Fu^{1,2} and Xiang-Dong Li^{1,2}

¹*Department of Astronomy, Nanjing University, Nanjing 210093, China; lixd@nju.edu.cn*

²*Key laboratory of Modern Astronomy and Astrophysics (Nanjing University), Ministry of Education, Nanjing 210093, China*

ABSTRACT

The spin evolution of isolated neutron stars (NSs) is dominated by their magnetic fields. The measured braking indices of young NSs show that the spin-down mechanism due to magnetic dipole radiation with constant magnetic fields is inadequate. Assuming that the NS magnetic field is buried by supernova fallback matter and re-emerges after accretion stops, we carry out Monte-Carlo simulation of the evolution of young NSs, and show that most of the pulsars have the braking indices ranging from -1 to 3 . The results are compatible with the observational data of NSs associated with supernova remnants. They also suggest that the initial spin periods of NSs might occupy a relatively wide range.

Subject headings: accretion, accretion disks – pulsars: general – stars: neutron – stars: magnetic fields

1. Introduction

The spin evolution is one of the most outstanding problems in pulsar astronomy. In the classical models the spin-down of isolated pulsars is due to the energy loss caused by magnetic dipole radiation, which is described as

$$I\dot{\Omega} = -\frac{B^2 R^6 \Omega^3}{6c^3}, \quad (1)$$

where Ω , $\dot{\Omega}$, I , B , and R are the angular velocity and its derivative, the moment of inertia, the surface magnetic field strength, and the radius of the pulsar, respectively, c is the speed of light. In realistic case the pulsar's spin-down may deviate from that due to pure dipole radiation, and a more general power-law form is adopted,

$$\dot{\Omega} = -K\Omega^n, \quad (2)$$

where K is a coefficient proportional to the spin-down torque, and the power-law index n is the so-called braking index. For a constant K , $n \equiv \Omega \ddot{\Omega} / \dot{\Omega}^2$. The initial spin period P_0 of the pulsar can be obtained by using Eq. (2) once the real spin-down age and the historically averaged braking index is known,

$$P_0 = \left[P^{n-1} - (n-1) \dot{P} T / P^{2-n} \right]^{1/(n-1)}, \quad (3)$$

where P ($\equiv \Omega/2\pi$), \dot{P} , and T are the current period, the period derivative, and the age of the pulsar, respectively.

So far, due to the uncertainties in timing measurements (e.g. timing noise and glitches) which usually dominate the relatively small values of the second derivative of Ω , it is impossible to measure the stable braking indices for the majority of pulsars (Kaspi et al. 1994). Only for those pulsars with relatively stable long-term spin-down, the secular braking indices have been measured. By using 23 year timing data Lyne et al. (1993) first obtained the braking index of the Crab pulsar (B0531+21) to be $n = 2.51(1)$, for which the time evolution of $\dot{\Omega}$ has been monitored for more than 40 years. The braking index of the Vela pulsar B0833–45 was measured by Lyne et al. (1996) to be $n = 1.4 \pm 0.2$, which is significantly less than the value expected in the magnetic dipole radiation model, indicating possible changes of the magnetic moment and/or the effective moment of inertia. Currently the braking indices have been measured in 13 pulsars (see Espinoza 2013, and references therein). Except PSRs J0537–6910 and B1757–24 which have negative n , other pulsars all have $0 < n < 3$. The smallest one is $n = 0.9 \pm 0.2$ for PSR J1734–3333 (Espinoza et al. 2011), which has a spin period of $P = 1.17$ s and a large period derivative $\dot{P} = 2.3 \times 10^{-12}$ ss $^{-1}$. The deduced magnetic field strength $B \simeq 5 \times 10^{13}$ G makes it among the highest B pulsars, and similar to those of magnetars (Olausen et al. 2013). The low n has been attributed to an increase of the dipole component of its magnetic field (Espinoza et al. 2011).

The possible reasons for the deviation of n from 3 have been studied extensively. They include, e.g., the pulsar wind in which the high-speed particles take the angular momentum away from the pulsar (Manchester & Taylor 1977), the distortion of the magnetic field from a pure dipole field (e.g. Barsukov & Tsygan 2010) and a oblique rotator in which the magnetic axis is misaligned with the axis of rotation (e.g. Contopoulos & Spitkovsky 2006). In particular, to explain that most of the measured values are less than 3, there are models invoking magnetic field increase (e.g. Blandford & Romani 1988) or fallback disk assisted spin-down (e.g. Marsden et al. 2001; Menou et al. 2001; Alpar et al. 2001; Chen & Li 2006) in young pulsars.

The growth of magnetic field in young neutron stars (NSs) may be caused by the re-emergence of the magnetic field (e.g. Muslimov & Page 1996; Geppert et al. 1999; Pons & Geppert

2007; Ho 2011; Bernal et al. 2013; Pons et al. 2012), which is buried due to the hypercritical accretion after the supernova events (Romani 1990). The re-emergence timescale depends on the total amount of accreted matter, which is $\sim 10^3 - 10^4$ yr for total accreted masses $\sim 10^{-4} - 10^{-3} M_{\odot}$. Relatively weak magnetic fields ($\sim 10^{10} - 10^{11}$ G) have been measured in a few young NSs in supernova remnants (SNRs) named central compact objects (CCOs) (Gotthelf et al. 2013, and references therein), which might have experienced the field burial and re-emergence process (Ho 2013).

Spin evolution of NSs with a surrounding fallback disk originated from the SN ejecta has been investigated by many authors (e.g. Chatterjee et al. 2000; Alpar 2001; Menou et al. 2001; Ertan et al. 2009; Yan et al. 2012). In these studies the NS magnetic fields were usually assumed to be constant, neglecting their possible evolution during and after the disk accretion. In this paper we use a Monte-Carlo method to calculate the evolution of young NSs. We assume that there is a fallback disk around all newborn NSs. Depending on the accreted mass the NS magnetic fields decay to some extent, and turn back to increase after accretion stops. By taking into account the disk accretion and field evolution simultaneously, we model the evolution of the spin periods and the braking indices of the NSs. We also compare the calculated distributions of various parameters with those derived from observations of young NSs.

The structure of this paper is as follows. We introduce the fallback disk model in Section 2, and describe the evolution of the magnetic field and the spin period of NSs, which is coupled with fallback disk accretion in Section 3. We present the calculated results of our population synthesis in Section 4. Discussion and conclusions are given in Section 5.

2. The fallback disk mass transfer

2.1. Time-evolution of a fallback disk

The SN fallback material is assumed to form from the metal-rich ejecta of core collapse SNe (Michel 1988; Chevalier 1989). The formation of a fallback disk requires that at least part of the fallback material possesses sufficient angular momentum. Compared with the accretion disks in binaries, the lifetime of which may be comparable with the evolutionary timescale of the binary or the donor star, the fallback disk has much shorter duration. The first possible detection of the fallback disk was made by Wang et al. (2006), who reported the mid-infrared counterpart of the anomalous X-ray pulsar (AXP) 4U 0142+61, and interpreted this as a passive dust fallback disk outside the pulsar’s magnetosphere heated by X-ray irradiation. Here we are not concerned with the formation processes of the fallback disk

which is rather complicated, but focus on its time-evolution.

The time dependence of the mass transfer rate of the disk and the size of a fallback disk was studied before (e.g. Menou et al. 2001; Ekş1 & Alpar 2003; Ertan et al. 2009; Cannizzo et al. 1990). Based on the self-similar solution of the standard thin disk (Shakura & Sunyaev 1973; Pringle 1981) the evolution of the mass transfer rate at the outer annulus of the disk \dot{M}_{tr} and the outer disk radius R_{d} can be written in the following form

$$\dot{M}_{\text{tr}}(t) = \dot{M}_0 (1 + t/t_0)^{-\alpha}, \quad (4)$$

$$R_{\text{d}}(t) = R_0 (1 + t/t_0)^{2\alpha-2}, \quad (5)$$

where the power exponent α is 5/4 for the opacity dominated by bound-free absorption, R_0 and \dot{M}_0 are the initial radius and mass transfer rate of the disk, respectively. t_0 is the timescale of disk formation, and is usually taken to be the dynamical timescale for the disk (Menou et al. 2001),

$$t_{\text{d}} \simeq 6.6 \times 10^{-5} T_{\text{c},6}^{-1} R_{0,8}^{1/2} \text{ yr}. \quad (6)$$

where $R_{0,8}$ and $T_{\text{c},6}$ are the initial outer disk radius in units of 10^8 cm and the temperature at R_{d} in units of 10^6 K (taken to be 1 in this paper), respectively. However, Ertan et al. (2009) showed that t_0 is more likely to be close to the viscous timescale in the disk,

$$t_{\text{v}} \simeq 3.19 \times 10^{-4} (M_0/10^{-4} M_{\odot})^{-3/7} R_{0,8}^{25/14} \text{ yr}, \quad (7)$$

where $M_0 = \int_0^{\infty} \dot{M}_{\text{tr}}(t) dt = \dot{M}_0 t_0 / (\alpha - 1)$ is the initial disk mass, or

$$t_{\text{v}} \simeq 2.58 \times 10^{-4} (\dot{M}_0/10^{25} \text{ g s}^{-1})^{-3/10} R_{0,8}^{5/4} \text{ yr}. \quad (8)$$

In our calculation we assign the maximum value of t_{d} and t_{v} to t_0 .

Since the temperature of the disk always decreases with time, at the later stage the outer regions of the disk may become neutral and passive (Menou et al. 2001; Ertan et al. 2009). However, it was argued that the irradiation by the NSs may be able to keep the disk ionized and prohibit the transition from an active to a passive disk (Alpar et al. 2001). Further calculation showed that the critical temperature T_{p} corresponding to the lowest ionization fraction that can generate viscosity in the disk is as low as $T_{\text{p}} \sim 100$ K (Alpar et al. 2013). Thus in this work we do not consider the neutralization process in the fallback disk.

2.2. Mass transfer and accretion

It is noted that the fallback disk accretion process is likely to be non-conservative. For a NS with a typical mass of $M = 1.4M_{\odot}$ the accretion rate (\dot{M}_{acc}) is generally limited by the

Eddington accretion rate $\dot{M}_E \simeq 10^{18} \text{g s}^{-1} \simeq 10^{-8} M_\odot \text{yr}^{-1}$. The initial transfer rate of the fallback material to the central object can be hypercritical and greatly exceed the Eddington limit. For example, in the case of SN 1987A, Chevalier (1989) suggested that the transfer rate at the time of reverse shock is $\sim 2.2 \times 10^{28} \text{g s}^{-1}$. More recently, Zhang et al. (2008) studied the supernova fallback for a wide range of progenitor masses and various metallicities and explosion energies. The transfer rate was also found to be $\sim 10^{29} \text{g s}^{-1}$ at the early phase. Note that this hypercritical accretion usually lasts very short time (less than 1 yr) compared to the spin evolution time of NSs. Super-Eddington accretion disks are likely to be advective and emit a wind. In the adiabatic inflow-outflow solutions (ADIOS) the mass transfer rate varies radially as $\dot{M}(r) \sim \dot{M}_{\text{tr}}(r/R_d)^p$ with $0 \leq p \leq 1$ (Blandford & Begelman 1999). The case $p = 0$ corresponds to the absence of a wind, while $p = 1$ implies strong mass loss, and the mass transfer rate at the inner edge \dot{M}_{in} is then not equal to \dot{M}_{tr} . A convenient form to relate the two rates is as follows,

$$\dot{M}_{\text{in}} = \begin{cases} \dot{M}_E (\dot{M}_{\text{tr}}/\dot{M}_E)^s, & \text{for } \dot{M}_{\text{tr}} > \dot{M}_E, \\ \dot{M}_{\text{tr}}, & \text{for } \dot{M}_{\text{tr}} \leq \dot{M}_E, \end{cases} \quad (9)$$

with $0 \leq s \leq 1$. For example, if $s = 0.75$, an initial \dot{M}_{in} distributed between 10^{25}gs^{-1} and 10^{28}gs^{-1} (as used below) corresponds to a \dot{M}_0 between $2 \times 10^{27} \text{gs}^{-1}$ and $2 \times 10^{31} \text{gs}^{-1}$, or the fallback mass between $4 \times 10^{-6} M_\odot$ and $0.04 M_\odot$ for typical disk formation time of about 1 s. Since the value of s (or p) is highly uncertain and it is unclear how much of the wind matter really leaves the system or falls back again to the disk, we don't consider the winds from the fallback disk for simplicity (i.e., $s = 1$ or $p = 0$), except the mass loss due to the Eddington limit accretion. In this case the accretion rate \dot{M}_{acc} of the NS is usually assumed to be $\dot{M}_{\text{acc}} = \min[\dot{M}_E, \dot{M}_{\text{in}}]$. However, if the photon's optical depth is too high, the radiation is trapped within a radius at which the outward diffusion luminosity equals the inward convected luminosity, so that the neutrino loss plays a crucial role, and the radiative transfer probably only dominates in the later evolution (Colgate 1971; Chevalier 1989). Chevalier (1989) showed that when the mass transfer rate decreases to $\dot{M}_{\text{cr}} \simeq 3 \times 10^{-4} M_\odot \text{yr}^{-1}$ the trapped photons can escape from the shocked envelope and the Eddington limit is enabled. Thus we assume that above this value the transferred mass is all accreted by the NS. The accretion rate of the NS can be formulated as

$$\dot{M}_{\text{acc}} = \begin{cases} \dot{M}_{\text{in}}, & \text{for } \dot{M}_{\text{in}} > \dot{M}_{\text{cr}} \text{ or } \dot{M}_{\text{in}} < \dot{M}_E, \\ \dot{M}_E, & \text{for } \dot{M}_E \leq \dot{M}_{\text{in}} \leq \dot{M}_{\text{cr}}. \end{cases} \quad (10)$$

3. Spin and magnetic field evolution of NSs

3.1. Spin evolution of NSs with a fallback disk

The spin evolution of NSs with a fallback disk can be divided into three phases according to the relationship of the following three critical radii.

(1) The magnetospheric radius R_m , at which the ram pressure of the accretion flow equals the magnetic pressure. Here we assume (Ghosh & Lamb 1979)

$$R_m = 0.5R_A = 0.5\left(\frac{B^2 R^6}{\dot{M}_{\text{in}}\sqrt{2GM}}\right)^{2/7},$$

where R_A is the Alfvén radius, and G is the gravitational constant. Note that if the mass transfer rate is sufficiently high R_m may be smaller than the NS radius R . This is physically impossible thus in our calculation we use

$$R_m = \max(R, 0.5R_A)$$

as the value of magnetospheric radius.

(2) The corotation radius

$$R_{\text{co}} = (GM/\Omega^2)^{1/3},$$

at which the Keplerian angular velocity of the disk is equal to that of the NS.

(3) The light cylinder radius

$$R_{\text{LC}} = c/\Omega,$$

at which the corotating extension of the NS is equal to the speed of light c .

We assumed that the pulsar activity is switched off and a disk torque is exerted on the NS when the disk is able to penetrate into the light cylinder (i.e., $R_m < R_{\text{LC}}$). Furthermore, if $R_m < R_{\text{co}}$ the NS is in the accretor phase, otherwise the accretion flow is stopped and ejected by the centrifugal barrier and the NS is in the propeller phase (Illarionov & Sunyaev 1975). The (unified) disk torque exerted on the NS in these two cases is taken to be (Menou et al. 2001),

$$I\dot{\Omega} = 2\dot{M}_{\text{acc}}R_m^2\Omega_{\text{K}}(R_m)[1 - \Omega/\Omega_{\text{K}}(R_m)], \quad (11)$$

where Ω_{K} is the Keplerian angular velocity in the disk. The NS is spun-up when $\Omega < \Omega_{\text{K}}(R_m)$ and spun-down when $\Omega > \Omega_{\text{K}}(R_m)$. When $\Omega = \Omega_{\text{K}}(R_m)$ the NS is spinning at the so-called “equilibrium period” given by

$$P_{\text{eq}} = 2\pi \left(\frac{R_m^3}{GM}\right)^{1/2}. \quad (12)$$

If $R_m \geq R_{LC}$ the pulsar activity starts to work, and the NS is in the ejector phase. Since the kinetic energy density in the disk has a radial dependence $\propto r^{-5/2}$ (where r is the distance from the center of the NS) steeper than the electromagnetic energy density outside the light cylinder ($\propto r^{-2}$), stable equilibrium of the disk outside the light cylinder is not allowed, unless it is beyond the gravitational capture radius (Lipunov et al. 1992). So in this case we consider the spin-down torque only due to magnetic dipole radiation*.

As the pulsar ages the radio luminosity will fade away, and finally it will become unobservable as a pulsating source. This is assumed to occur when its evolutionary track on the $B - P$ plane crosses the so-called death-line given by (Ruderman & Sutherland 1975)

$$B = 0.17 \times 10^{12} P^2 \text{ G}. \quad (13)$$

3.2. Magnetic field evolution

Magnetic field is the most important parameter that determines the spin evolution and the observational properties of isolated NSs. We assume that, along with accretion, the NS magnetic fields decay with the following form (Taam & van den Heuvel 1986; Shibasaki et al. 1989):

$$B = \frac{B_0}{1 + \Delta M / 10^{-5} M_\odot}, \quad (14)$$

where B_0 is the initial magnetic field and ΔM is the accreted mass. When accretion stops the buried field will re-diffuse to the surface due to Ohmic diffusion and Hall drift (e.g., Geppert et al. 1999). The field diffusion process is governed by the MHD induction equation, and its speed depends on the initial magnetic strength and the overall accreted mass (for recent reviews, see Geppert 2009; Ho 2013). Based on the numerical calculations of field re-diffusion (e.g. Geppert et al. 1999; Ho 2011), we fit the results with a phenomenological law for the growth rate of the magnetic field after accretion,

$$\dot{B} = 0.01 \left(\frac{\Delta M}{M_\odot} \right)^{-3} \left(1 - \frac{B}{B_0} \right)^2 \text{ G yr}^{-1}. \quad (15)$$

Figure 1 illustrates the field emergence with different accreted mass.

*This is different from Menou et al. (2001) and Yan et al. (2012), who assumed that even in the ejector phase the disk can still exist outside the light cylinder, and the inner radius of the disk always coincides with the light cylinder radius irrespective of the decreasing mass transfer rate.

4. Synthesis of NS population

In our Monte-Carlo simulation of the NS population we adopt similar input parameters as in Yan et al. (2012). In previously works, the distribution of the birth spin periods of NSs has been suggested to be in a wide range from several milliseconds to hundreds of milliseconds (e.g. Arzoumanian et al. 2002; Faucher-Giguère & Kaspi 2006), with various forms, e.g., a fix value (e.g. Fan et al. 2001), a flat distribution (e.g. Kiel et al. 2008), and a (logarithm) Gaussian distribution (e.g. Regimbau & de Freitas Pacheco 2001; Lorimer et al. 1993). The SNRs may present useful constraints on the initial spins of the pulsars associated with them. There is evidence supporting that the NSs are born with both fast and slow rotation. For example, the initial spin period (~ 19 ms) of the Crab pulsar estimated from the age of the Crab nebula and the measured braking index (Manchester & Taylor 1977) implies that the NS was born spinning rapidly. The CCO 1E 1207.4–5209 in the SNR G296.5+10.0 has a spin period of 0.424 s (Zavlin et al. 2000) and period derivative $\dot{P} < 2.5 \times 10^{-16} \text{ ss}^{-1}$ (Gotthelf & Halpern 2007). The characteristic age of the NS $\tau_c > 27$ Myr exceeding the age of the SNR by three orders of magnitude, suggesting that 1E 1207.4–5209 was born with a spin period very similar to the current value. Here we adopt three different distributions of the initial spin periods, i.e., the “fast” population with,

$$\langle \log P_0(\text{s}) \rangle = -2.3, \quad \sigma_{\log P_0} = 0.3, \quad (16)$$

the “slow” spin population with

$$\langle \log P_0(\text{s}) \rangle = -0.5, \quad \sigma_{\log P_0} = 0.2, \quad (17)$$

and the “composite” population in which we assume that $\sim 40\%$ of the pulsars are born in the slow population (Vranesevic et al. 2004).

For the initial magnetic field almost all the works adopted a logarithm Gaussian distribution, and we take the following form of Arzoumanian et al. (2002):

$$\langle \log B_0(\text{G}) \rangle = 12.35, \quad \sigma_{\log B_0} = 0.4. \quad (18)$$

We follow Yan et al. (2012) to assume a logarithm uniform distribution of the initial mass transfer rate \dot{M}_0 ranging from 10^{25} to 10^{28} g s^{-1} , which is roughly consistent with previous semi-analytical and numerical results (Chevalier 1989; MacFadyen et al. 2001; Mineshige et al. 1997; Zhang et al. 2008). The initial radius of the fallback disk depends on the specific angular momentum of the fallback material. At the pre-supernova stage the specific angular momentum of the iron core of a rapidly rotating star with mass $8 - 25M_\odot$ is $\sim 10^{16} - 10^{17} \text{ cm}^2 \text{ s}^{-1}$ (see Heger et al. 2000), corresponding a circularization radius \sim

$10^6 - 10^8$ cm. Thus we randomly select the logarithm of the initial radius (in units of cm) between 6 and 8.

Figures 2-4 illustrate the evolution of NSs with different initial parameters. Here we take typical values for the mass ($1.4M_\odot$), radius (10^6 cm) and initial magnetic field ($\sim 2 \times 10^{12}$ G) of the NS. The braking index n and characteristic age τ are plotted throughout the evolution although they are measurable only in the ejector phase. We consider three cases, in two of which \dot{M}_0 and R_0 are close to the maximum and minimum of the adopted values (note that t_v and t_d are positively correlated with R_0), and in third one we choose the medium values for \dot{M}_0 and R_0 . In each figure the initial spin period is taken to be $P_0 = 300$ ms and 5 ms in the left and right panels, and the accretor, propeller and ejector phases are shown in dotted, dashed and solid lines, respectively.

In Fig. 2 we set $\dot{M}_0 = 10^{28} \text{ gs}^{-1}$ and $R_0 = 10^8$ cm for NSs with both fast and slow initial spins. The magnetic field decays to be below 10^9 G within ~ 0.1 yr as $\sim 4 \times 10^{-2} M_\odot$ mass is accreted, and has not recovered to its initial value at 10^6 yr. In the left panel the NS is correspondingly accelerated from 300 ms to ~ 4 ms within the first ~ 0.1 yr. The accretor phase lasts $\sim 10^5$ yr, followed by the propeller phase until 10^6 yr. The time dependence of n and τ_c is more complicated, which vary drastically during the evolution. At the beginning of the evolution, due to the enormously high accretion rate, the magnetosphere radius is suppressed to the NS surface. In this early stage $n < 0$ since $\ddot{\Omega} < 0$. When \dot{M}_{in} decreases to be lower than \dot{M}_{cr} , \dot{M}_{acc} is limited by the Eddington limit. At this time R_m is still equal to R (note that R_m depends on \dot{M}_{in}), and $\dot{\Omega}$ is nearly constant, thus $n \sim 0$. As \dot{M}_{in} continues to decrease R_m becomes larger than R , and n rapidly rises to ~ 50 because $\dot{R}_m > 0$ and $\ddot{M}_{\text{acc}} \sim 0$ at this time. When $\dot{M}_{\text{in}} = \dot{M}_{\text{E}}$, n has another abrupt change. At this time \ddot{M}_{acc} dominates over \dot{R}_m and $n < 0$. When \dot{M}_{acc} decreases so that $R_m = R_{\text{co}}$ the NS enters the propeller phase, and the evolution is stopped at 10^6 year.

In Fig. 3 we set moderate values for $\dot{M}_0 (= 10^{27} \text{ gs}^{-1})$ and $R_0 (= 10^7 \text{ cm})$. Since the accreted mass ($\sim 10^{-3} M_\odot$) is significantly lower than in Fig. 2, the magnetic field first decays to a few 10^{10} G, and re-grows to its initial value within 10^6 yr. The fast-spinning NS has experienced all three evolutionary phases while the slow one is still in the propeller phase at the age of 10^6 yr. In Fig. 4 we take $\dot{M}_0 = 10^{25} \text{ gs}^{-1}$ and $R_0 = 2 \times 10^6$ cm (we note that if $R_0 = 10^6$ cm, R_m is larger than R_0 at the beginning of the evolution, the fallback disk does not exist and the NS enters the ejector phase directly). With such a low mass transfer rate the accretor phase is very short, about 2 yr and 10^{-3} yr for slow and rapid spinning NSs, respectively. The ejector phase correspondingly starts at around 10^4 yr and 0.1 yr.

As we are only concerned with young pulsars, in the Monte-Carlo simulation we generate 100 NSs every 100 years in the first 10^4 years, and extrapolate the results to 10^6 years by

sampling the parameters of NSs every 10^4 years during the calculation. The distributions of P and B of the NS population are plotted in Fig. 5, at the time when the NS enters the pulsar phase, and of 10^4 yr and 10^6 yr. Note that here “pulsars” mean NSs in the ejector phase and located above the death line in the $B - P$ diagram. The calculated P distribution at 10^6 years shows double-peak structure for both the fast and slow spin populations. The reason is as follows. When the initial mass transfer rate is high, the NS magnetic field is decayed by several orders of magnitude, and the NS spends most of the time (several 10^5 yr) in the accretor and propeller phases. Because of the weak magnetic field, the spin-down induced by the propeller torque and magnetic dipole radiation is insignificant, giving rise to a group of rapidly spinning pulsars in both the fast and slow population. The distribution of the composite population is a hybrid of the fast and slow population and has multi-peak structure at 10^6 yr. For the fast spin population the distributions of P and B at 10^4 yr provide a natural transition between the initial pulsar state to the relatively old one (at 10^6 yr). However it is not the case in the slow spin population because, unlike the fast spin population in which most NSs have evolved into the ejector phase at 10^4 yr, many of the slow NSs are still in the accretor and propeller phases.

In order to show the distribution of the braking indices and the characteristic ages for pulsars with different ages, we adopt the same initial distribution of the parameters as in the previous simulations but a variable birth rate, to ensure that the total number of NSs is constant for every logarithm interval of the age (see also Yan et al. 2012). For example, for ages between $10 - 10^2$ yr, $10^2 - 10^3$ yr and $10^3 - 10^4$ yr the birth rate is taken to be 1 yr^{-1} , 10^{-1} yr^{-1} and 10^{-2} yr^{-1} respectively. Figure 6 shows the distributions of τ_c and n versus the age. The green and red crosses represent the NSs as observable pulsars and in the accretor/propeller phase, respectively. It is seen that for the slow spin population very few NSs can enter the pulsar phase within 10^6 years.

For comparison with observations we also plot the observational data of pulsars with dots (with error bars) in Fig. 6. Here the pulsars are those associated with SNRs and with measured braking indices. The samples of SNR-PSR associations are taken from the ATNF pulsar catalogue[†] and a census of high-energy observations of the Galactic SNRs[‡] (Manchester et al. 2005; Safi-Harb et al. 2013). Thus we use the SNR ages as the real ages of the pulsars. The parameters of these pulsars are listed in Table 1.

For all the three populations, the characteristic ages of the pulsars usually exceed their real ages by a factor up to $\sim 10^3$. The braking indices concentrate in the range $-1 < n < 3$

[†]<http://www.atnf.csiro.au/people/pulsar/psrcat/>

[‡]<http://www.physics.umanitoba.ca/snr/SNRcat/>

which is consistent with observations, but they can reach $\sim -10^3$. There is no pulsar with $n > 3$, since in our model NSs with $n > 3$ are in the accretor or propeller phase and thus unobservable, and the magnetic field growth is the only cause for the variation of n . Actually the braking indices for NSs in accretor and propeller phase are distributed in a much wider range of $[-10^5, 10^3]$.

5. Discussion and conclusions

We have carried out population synthesis calculations of the NS evolution, taking into account the supernova fallback accretion, which suppresses the NS magnetic fields, and the post-emergence of the buried field. Though the input parameters in our simulation are similar to those in Yan et al. (2012), some of the important assumptions are different in the two works. First, Yan et al. (2012) assume that a fallback disk always surrounds the NS and exerts a torque on it; in our model the evolutionary sequence of the NS is divided into the accretor, propeller and ejector phases, the disk torque works only in the accretor and propeller phases, and the NS acts as a pulsar only in the ejector phase. Second, we consider the hypercritical accretion from the fallback matter when $\dot{M}_{\text{in}} > \dot{M}_{\text{cr}}$, and include the magnetic field evolution during and after the accretion, while in Yan et al. (2012) the mass accretion rate is limited by \dot{M}_{E} and the magnetic field is assumed to be constant. Third, for the disk evolution we take the formation time $t_0 = \max(t_v, t_d)$ rather $t_0 = t_d$ as in Yan et al. (2012). This results in a lower mass transfer rate in the disk at the same age in our case. In our work due to the magnetic field re-emergence n is always smaller than 3 when the NS is in the ejector phase, while in Yan et al. (2012) the deviation of n from 3 is caused by the disk torque: the majority of the pulsars have $n < 3$, but a considerable fraction of them have $n > 3$ (especially for the slow spin population). The distributions of both τ_c and n in our work are more dispersed and extended than in Yan et al. (2012), since the magnetic field usually evolves on a longer timescale than the fallback disk.

Figure 6 shows that the statistical results of the fast spin population seem to be compatible with the observed distribution of the braking indices and the ages of young pulsars. NSs born with slow spins are difficult to survive the accretor and propeller phases. On the other hand, the birth period distribution for pulsars may also present possible constraints on the initial period distribution of the NSs[§]. Recently Noutsos et al. (2013) derived the kinematic ages for 52 pulsars based on the measured pulsar proper motions and positions,

[§]Note that the birth periods of pulsars are the initial periods when the NSs enter the ejector phase. They are similar to but not identical with the initial periods of newborn NSs.

by modelling the trajectory of the pulsars in a Galactic potential. They found that the birth periods of these pulsars show two-population structure, one with $P_0 < 400$ ms and the other with $700 \text{ ms} < P_0 < 1.1$ s. Although this result is based on the standard magnetic-dipole braking ($n = 3$), it is unlikely to deviate far from the real situation as shown by the authors. If we compare their birth period distribution with our calculated results (Fig. 5), we find that a considerable fraction of NSs may be born with relatively slow spins. This suggests that the newborn NSs might be composed by composite populations with a wide range of the spin periods.

It should be noted that currently solid theories on SN fallback and related field evolution are lacking, and hence many parameters adopted in our model are quite uncertain. This means that our results can be only regarded as illustrative rather for real situation. However, they keep the basic features for the evolution of the braking indices and the relation between the characteristic ages and the real ages. The model may be **tested** or refined by future observations.

We do not consider late evolution of the NSs. As shown by Pons et al. (2012), the effect of the magnetic field evolution on the braking index can be divided into three qualitatively different stages, depending on the age and the internal temperature of the NS: a first stage with fallback accretion and subsequent field evolution ($n < 3$); in a second stage, the evolution is governed by almost pure Ohmic field decay, and a braking index $n > 3$ is expected; in the third stage, at late times, when the interior temperature has dropped to very low values, the Hall oscillatory modes in the NS crust result in braking indices of high absolute value and both positive and negative signs. In the model proposed by Zhang & Xie (2012) the field evolution is caused by a long-term power law decay coupled with short-term oscillations.

This work was supported by the Natural Science Foundation of China under grant numbers 11133001 and 11203009, the National Basic Research Program of China (973 Program 2009CB824800), and the Qinglan project of Jiangsu Province.

REFERENCES

- Abdo, A. A., Wood, K. S., DeCesar, M. E., et al. 2012, *ApJ*, 744, 146
- Albert, J., Aliu, E., Anderhub, H., et al. 2008, *ApJ*, 674, 1037
- Alpar, M. A. 2001, *ApJ*, 554, 1245
- Alpar, M. A., Ankay, A., & Yazgan, E. 2001, *ApJ*, 557, L61
- Alpar, M. A., Çalışkan, Ş., & Ertan, Ü. 2013, in *Feeding Compact Objects: Accretion on All Scales*, IAU Symposium, Vol. 290, ed. C. M. Zhang, T. Belloni, M. Méndez, & S. N. Zhang (Cambridge University Press), 93
- Arzoumanian, Z., Chernoff, D. F., & Cordes, J. M. 2002, *ApJ*, 568, 289
- Aschenbach, B., Egger, R., & Trümper, J. 1995, *Nature*, 373, 587
- Barsukov, D. P., & Tsygan, A. I. 2010, *MNRAS*, 409, 1077
- Becker, W., Prinz, T., Winkler, P. F., & Petre, R. 2012, *ApJ*, 755, 141
- Bernal, C. G., Page, D., & Lee, W. H. 2013, *ApJ*, 770, 106
- Bietenholz, M. F., & Bartel, N. 2008, *MNRAS*, 386, 1411
- Blandford, R. D., & Begelman, M. C. 1999, *MNRAS*, 303, L1
- Blandford, R. D., & Romani, R. W. 1988, *MNRAS*, 234, 57
- Bocchino, F., Bandiera, R., & Gelfand, J. 2010, *A&A*, 520, A71
- Camilo, F., Ng, C.-Y., Gaensler, B. M., et al. 2009, *ApJ*, 703, L55
- Cannizzo, J. K., Lee, H. M., & Goodman, J. 1990, *ApJ*, 351, 38
- Caswell, J. L., Kesteven, M. J., Komesaroff, M. M., et al. 1987, *MNRAS*, 225, 329
- Caswell, J. L., Kesteven, M. J., Stewart, R. T., Milne, D. K., & Haynes, R. F. 1992, *ApJ*, 399, L151
- Chatterjee, P., Hernquist, L., & Narayan, R. 2000, *ApJ*, 534, 373
- Chen, W. C. & Li, X. D. 2006, *A&A*, 450, L1
- Chevalier, R. A. 1989, *ApJ*, 346, 847

- Colgate, S. A. 1971, *ApJ*, 163, 221
- Contopoulos, I., & Spitkovsky, A. 2006, *ApJ*, 643, 1139
- Downes, A. J. B., Pauls, T., & Salter, C. J. 1980, *A&A*, 92, 47
- Ekşi, K. Y., & Alpar, M. A. 2003, *ApJ*, 599, 450
- Ertan, Ü., Ekşi, K. Y., Erkut, M. H., & Alpar, M. A. 2009, *ApJ*, 702, 1309
- Espinoza, C. M. 2013, in *Neutron Stars and Pulsars: Challenges and Opportunities after 80 years*, IAU Symposium, Vol. 291, ed. J. van Leeuwen (Cambridge University Press), 195
- Espinoza, C. M., Lyne, A. G., Kramer, M., Manchester, R. N., & Kaspi, V. M. 2011, *ApJ*, 741, L13
- Fan, G. L., Cheng, K. S., & Manchester, R. N. 2001, *ApJ*, 557, 297
- Fang, J. & Zhang, L. 2010a, *A&A*, 515, A20
- . 2010b, *ApJ*, 718, 467
- Faucher-Giguère, C.-A., & Kaspi, V. M. 2006, *ApJ*, 643, 332
- Fesen, R., Rudie, G., Hurford, A., & Soto, A. 2008, *ApJS*, 174, 379
- Finley, J. P., & Oegelman, H. 1994, *ApJ*, 434, L25
- Gaensler, B. M., Gotthelf, E. V., & Vasisht, G. 1999, *ApJ*, 526, L37
- Geppert, U. 2009, in *Astrophysics and Space Science Library*, Vol. 357, (Astrophysics and Space Science Library), ed. W. Becker, 319
- Geppert, U., Page, D., & Zannias, T. 1999, *A&A*, 345, 847
- Giacani, E., Smith, M. J. S., Dubner, G., et al. 2009, *A&A*, 507, 841
- Gotthelf, E. V., & Halpern, J. P. 2007, *ApJ*, 664, L35
- Gotthelf, E. V., & Halpern, J. P. 2008, in *40 Years of Pulsars: Millisecond Pulsars, Magnetars and More*, American Institute of Physics Conference Series, Vol. 983, ed. C. Bassa, Z. Wang, A. Cumming, & V. M. Kaspi, 320
- . 2009a, *ApJ*, 695, L35

- . 2009b, *ApJ*, 700, L158
- Gotthelf, E. V., Halpern, J. P., & Alford, J. 2013, *ApJ*, 765, 58
- Gotthelf, E. V., Vasisht, G., Boylan-Kolchin, M., & Torii, K. 2000, *ApJ*, 542, L37
- Hales, C. A., Gaensler, B. M., Chatterjee, S., van der Swaluw, E., & Camilo, F. 2009, *ApJ*, 706, 1316
- Heger, A., Langer, N., & Woosley, S. E. 2000, *ApJ*, 528, 368
- Ho, W. C. G. 2011, *MNRAS*, 414, 2567
- Ho, W. C. G. 2013, in *Neutron Stars and Pulsars: Challenges and Opportunities after 80 years*, IAU Symposium, Vol. 291, ed. J. van Leeuwen (Cambridge University Press), 101
- Hwang, U., Petre, R., Holt, S. S., & Szymkowiak, A. E. 2001, *ApJ*, 560, 742
- Illarionov, A. F., & Sunyaev, R. A. 1975, *A&A*, 39, 185
- Kargaltsev, O., & Pavlov, G. G. 2008, in *American Institute of Physics Conference Series, Vol. 983, 40 Years of Pulsars: Millisecond Pulsars, Magnetars and More*, ed. C. Bassa, Z. Wang, A. Cumming, & V. M. Kaspi, 171
- Kaspi, V. M., Manchester, R. N., Siegman, B., Johnston, S., & Lyne, A. G. 1994, *ApJ*, 422, L83
- Kaspi, V. M., Roberts, M. E., Vasisht, G., et al. 2001, *ApJ*, 560, 371
- Kiel, P. D., Hurley, J. R., Bailes, M., & Murray, J. R. 2008, *MNRAS*, 388, 393
- Koo, B.-C., & Heiles, C. 1995, *ApJ*, 442, 679
- Kothes, R. 2010, in *The Dynamic Interstellar Medium: A Celebration of the Canadian Galactic Plane Survey*, *Astronomical Society of the Pacific Conference Series*, Vol. 438, ed. R. Kothes, T. L. Landecker, & A. G. Willis (San Francisco: Astronomical Society of the Pacific), 347
- Kramer, M., Lyne, A. G., Hobbs, G., et al. 2003, *ApJ*, 593, L31
- Kumar, H. S., Safi-Harb, S., & Gonzalez, M. E. 2012, *ApJ*, 754, 96
- Leahy, D. A., & Ranasinghe, S. 2012, *MNRAS*, 423, 718

- Lin, L. C. C., Huang, R. H. H., Takata, J., et al. 2010, *ApJ*, 725, L1
- Lipunov, V. M., Börner, G., & Wadhwa, R. S. 1992, *Astrophysics of Neutron Stars* (Astronomy and Astrophysics Library)
- Livingstone, M. A., Kaspi, V. M., Gavriil, F. P., et al. 2007, *Ap&SS*, 308, 317
- Lorimer, D. R., Bailes, M., Dewey, R. J., & Harrison, P. A. 1993, *MNRAS*, 263, 403
- Lyne, A. G., Pritchard, R. S., & Graham-Smith, F. 1993, *MNRAS*, 265, 1003
- Lyne, A. G., Pritchard, R. S., Graham-Smith, F., & Camilo, F. 1996, *Nature*, 381, 497
- MacFadyen, A. I., Woosley, S. E., & Heger, A. 2001, *ApJ*, 550, 410
- Manchester, R. N., Hobbs, G. B., Teoh, A., & Hobbs, M. 2005, *AJ*, 129, 1993
- Manchester, R. N., & Taylor, J. H. 1977, *Pulsars* (W. H. Freeman & Co Ltd)
- Marsden, D., Lingenfelter, R. E., & Rothschild, R. E. 2001, *ApJ*, 547, L45
- Marthi, V. R., Chengalur, J. N., Gupta, Y., Dewangan, G. C., & Bhattacharya, D. 2011, *MNRAS*, 416, 2560
- Menou, K., Perna, R., & Hernquist, L. 2001, *ApJ*, 559, 1032
- Michel, F. C. 1988, *Nature*, 333, 644
- Middleditch, J., Marshall, F. E., Wang, Q. D., Gotthelf, E. V., & Zhang, W. 2006, *ApJ*, 652, 1531
- Mineshige, S., Nomura, H., Hirose, M., Nomoto, K., & Suzuki, T. 1997, *ApJ*, 489, 227
- Muslimov, A., & Page, D. 1996, *ApJ*, 458, 347
- Nicastro, L., Johnston, S., & Koribalski, B. 1996, *A&A*, 306, L49
- Noutsos, A., Schnitzeler, D. H. F. M., Keane, E. F., Kramer, M., & Johnston, S. 2013, *MNRAS*, 430, 2281
- Olausen, S. A., Zhu, W. W., Vogel, J. K., et al. 2013, *ApJ*, 764, 1
- Park, S., Burrows, D. N., Garmire, G. P., et al. 2003, *ApJ*, 586, 210
- Park, S., Hughes, J. P., Slane, P. O., Mori, K., & Burrows, D. N. 2010, *ApJ*, 710, 948

- Pons, J. A., & Geppert, U. 2007, *A&A*, 470, 303
- Pons, J. A., Viganò, D., & Geppert, U. 2012, *A&A*, 547, A9
- Pringle, J. E. 1981, *ARA&A*, 19, 137
- Regimbau, T., & de Freitas Pacheco, J. A. 2001, *A&A*, 374, 182
- Rho, J., & Borkowski, K. J. 2002, *ApJ*, 575, 201
- Roberts, M. S. E., & Brogan, C. L. 2008, *ApJ*, 681, 320
- Romani, R. W. 1990, *Nature*, 347, 741
- Roy, J., Gupta, Y., & Lewandowski, W. 2012, *MNRAS*, 424, 2213
- Ruderman, M. A., & Sutherland, P. G. 1975, *ApJ*, 196, 51
- Ruiz, M. T., & May, J. 1986, *ApJ*, 309, 667
- Safi-Harb, S., Ferrand, G., & Matheson, H. 2013, in *Neutron Stars and Pulsars: Challenges and Opportunities after 80 years*, IAU Symposium, Vol. 291, ed. J. van Leeuwen (Cambridge University Press), 483
- Sasaki, M., Plucinsky, P. P., Gaetz, T. J., et al. 2004, *ApJ*, 617, 322
- Shakura, N. I., & Sunyaev, R. A. 1973, *A&A*, 24, 337
- Shibazaki, N., Murakami, T., Shaham, J., & Nomoto, K. 1989, *Nature*, 342, 656
- Sun, M., Seward, F. D., Smith, R. K., & Slane, P. O. 2004, *ApJ*, 605, 742
- Taam, R. E., & van den Heuvel, E. P. J. 1986, *ApJ*, 305, 235
- Tam, C., & Roberts, M. S. E. 2003, *ApJ*, 598, L27
- Tian, W. W., & Leahy, D. A. 2006, *A&A*, 455, 1053
- Uchiyama, Y., Takahashi, T., Aharonian, F. A., & Mattox, J. R. 2002, *ApJ*, 571, 866
- Velázquez, P. F., Dubner, G. M., Goss, W. M., & Green, A. J. 2002, *AJ*, 124, 2145
- Vink, J., & Kuiper, L. 2006, *MNRAS*, 370, L14
- Vranesevic, N., Manchester, R. N., Lorimer, D. R., et al. 2004, *ApJ*, 617, L139
- Wang, Q. D., & Gotthelf, E. V. 1998, *ApJ*, 509, L109

- Wang, Z., Chakrabarty, D., & Kaplan, D. L. 2006, *Nature*, 440, 772
- Weltevrede, P., Johnston, S., & Espinoza, C. M. 2011, *MNRAS*, 411, 1917
- Winkler, P. F., Twelker, K., Reith, C. N., & Long, K. S. 2009, *ApJ*, 692, 1489
- Yan, T., Perna, R., & Soria, R. 2012, *MNRAS*, 423, 2451
- Yar-Uyaniker, A., Uyaniker, B., & Kothes, R. 2004, *ApJ*, 616, 247
- Zavlin, V. E., Pavlov, G. G., Sanwal, D., & Trümper, J. 2000, *ApJ*, 540, L25
- Zhang, S.-N., & Xie, Y. 2012, *ApJ*, 761, 102
- Zhang, W., Woosley, S. E., & Heger, A. 2008, *ApJ*, 679, 639

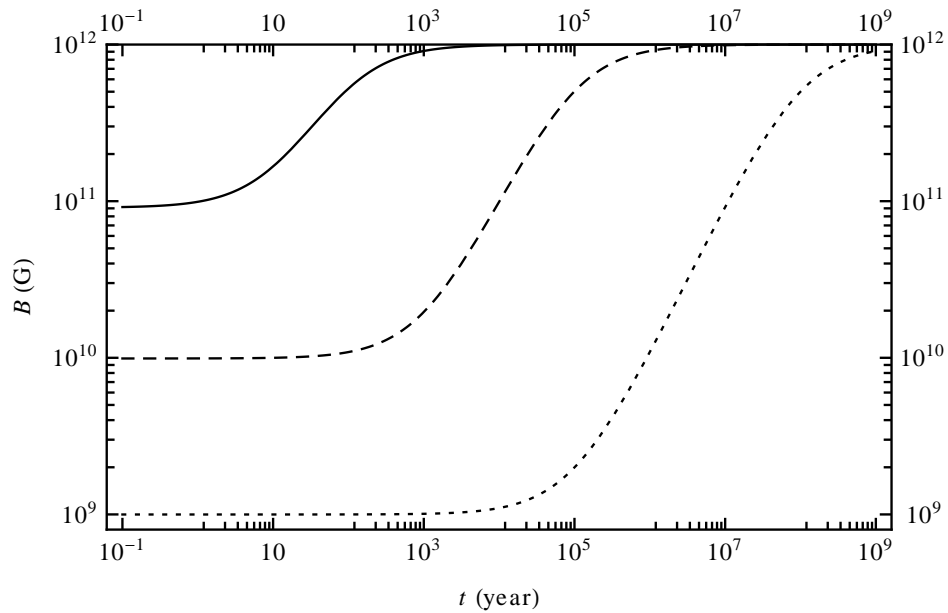


Fig. 1.— An illustration of the magnetic field emergence according to Eq. (15) for an initial magnetic field strength of $B_0 = 10^{12}$ G. The lines from top to bottom correspond to the accreted mass of 10^{-4} , 10^{-3} and $10^{-2} M_{\odot}$, respectively.

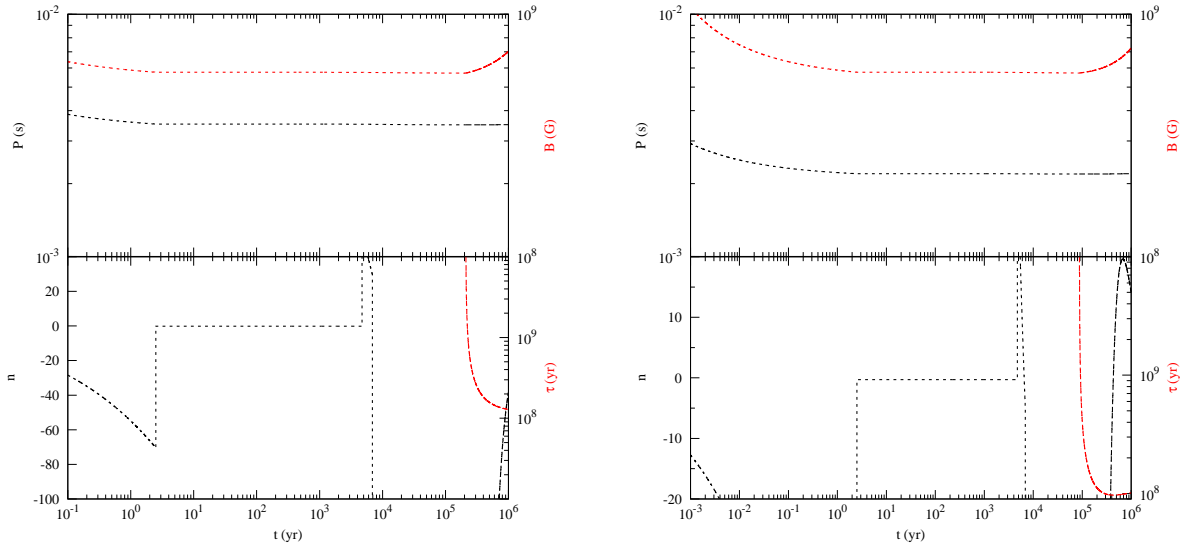


Fig. 2.— Evolution of the spin period P , the magnetic field B (top), the braking index n and the characteristic age τ (bottom) of a NS with an initial magnetic field of 2.24×10^{12} G. The initial spin period is taken to be $P_0 = 300$ ms and 5 ms in the left and right panels, respectively; in both panels we set $R_0 = 10^8$ cm and $\dot{M}_0 = 10^{28}$ g s $^{-1}$. In this and the following two figures, the curves for P and n are plotted in black, and for B and τ in red; the accretor, propeller and ejector phases are represented with dotted, dashed and solid lines, respectively.

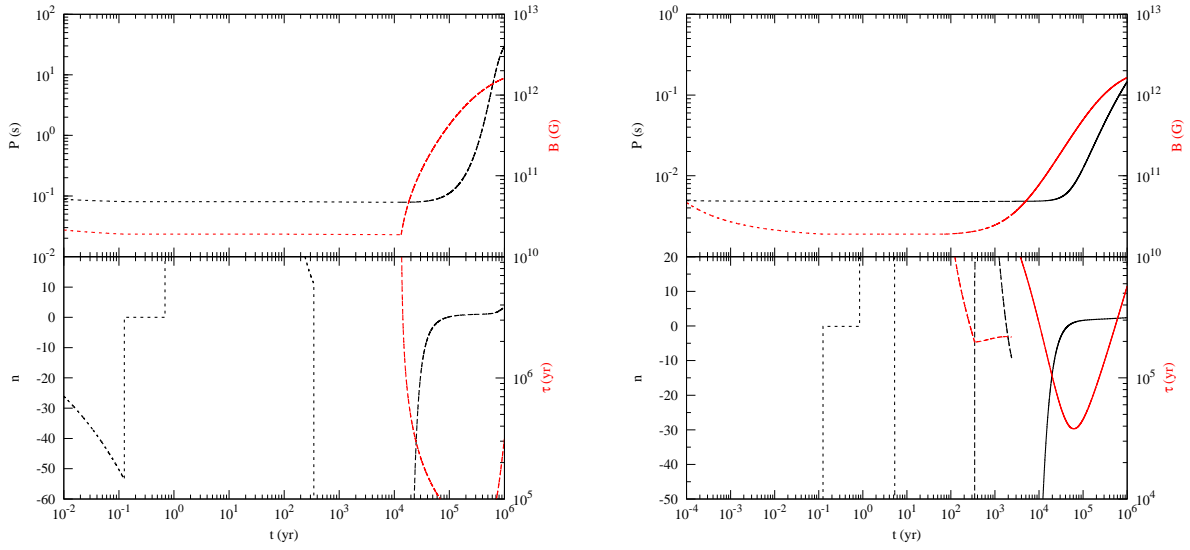


Fig. 3.— Same as Fig. 2 but for $R_0 = 10^7$ cm and $\dot{M}_0 = 10^{27}$ g s $^{-1}$.

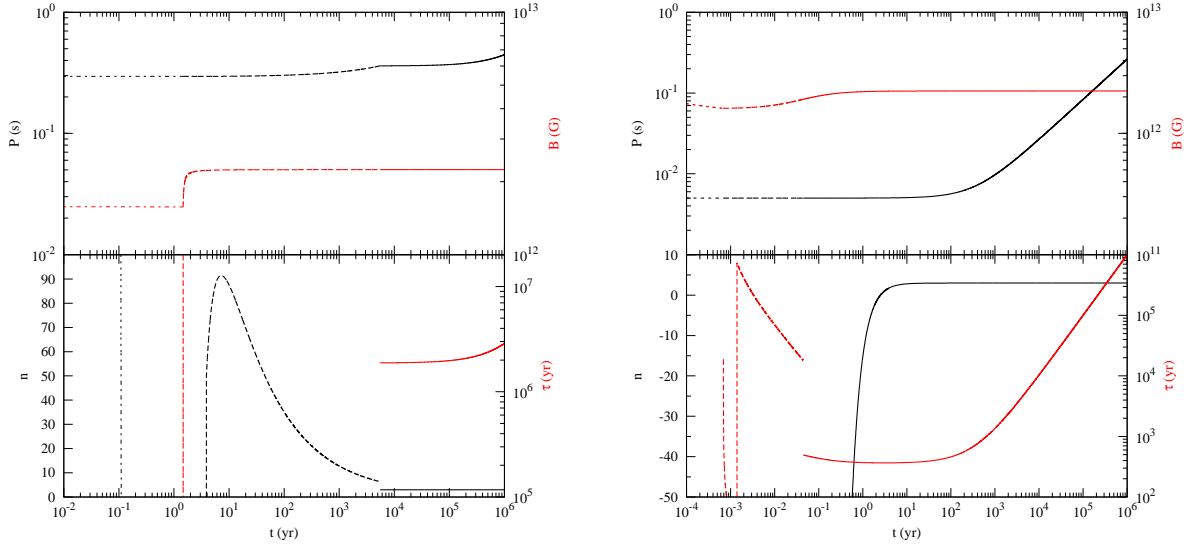


Fig. 4.— Same as Fig. 2 but for $R_0 = 2 \times 10^6$ cm and $\dot{M}_0 = 10^{25}$ g s $^{-1}$.

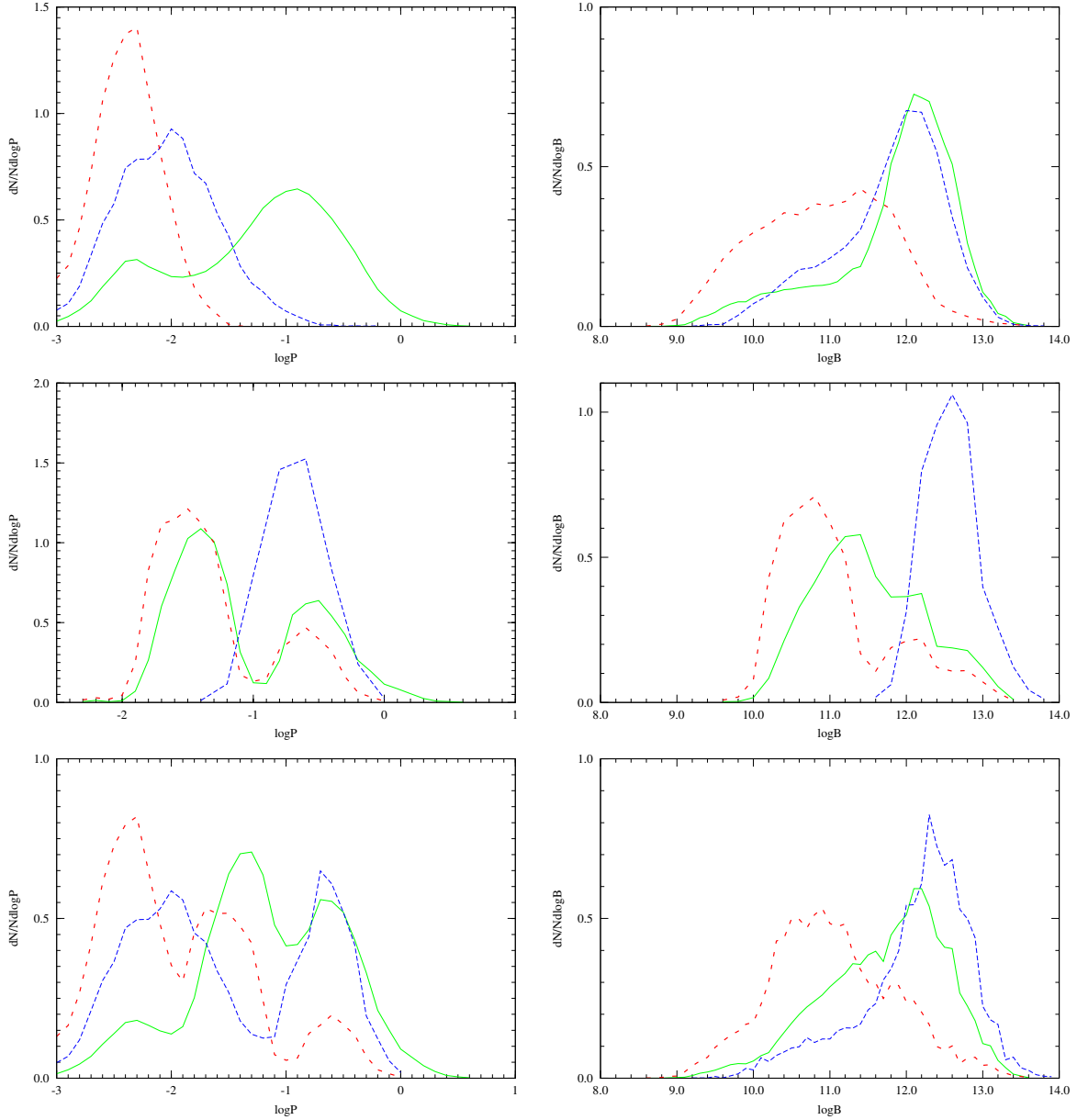


Fig. 5.— The distribution of the spin period P and the magnetic field B of the pulsars. From top to bottom panels are the fast, slow and composite spin populations, respectively. Dotted lines in red represent the distributions of the initial spin period and magnetic field of pulsars, i.e., when the NSs enter the ejector phase. Blue dashed and green solid lines are for the distributions of P and B of pulsars at 10^4 and 10^6 yr. The composite population is composed of 60% fast pulsars and 40% slow pulsars.

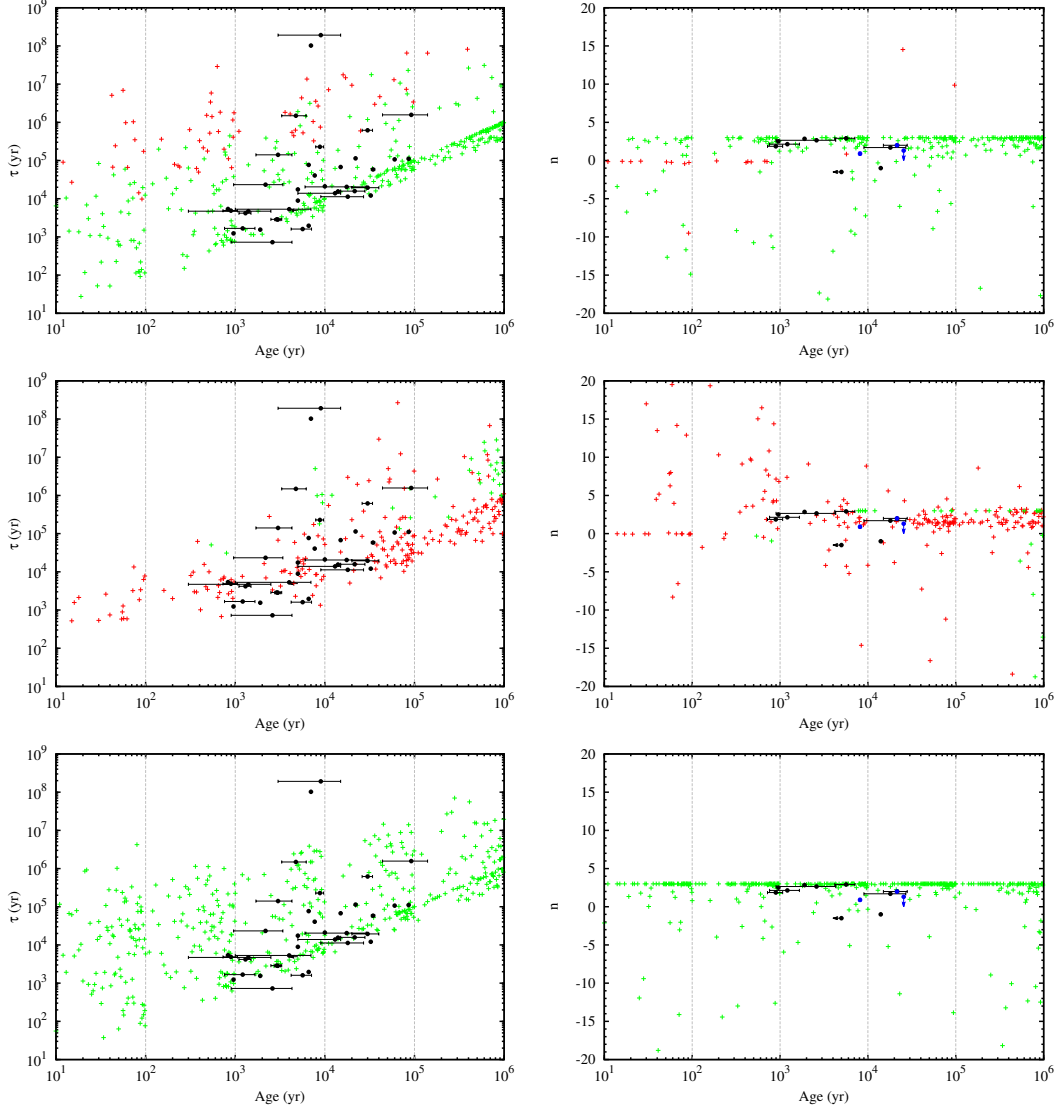


Fig. 6.— A comparison of the distribution of τ and n versus different NS ages. From the top to the bottom panels are the fast, slow and composite spin populations. NSs in the ejector phase are plotted in green crosses, those in the accretor and propeller phases are plotted in red crosses. NSs with measured braking indices and SNR associations are plotted in black dots with error bars. For NSs associated with SNRs we use the SNR age as the real age of the NS if the SNR age is available, except for PSRs J1734–3333, J1747–2958 and B1823–13, for which we use τ as the real age and plot with blue dots in the right panel. The composite spin population is composed of 60% fast pulsars and 40% slow pulsars.

Table 1. Parameters for pulsars with measured braking indices and/or associated with SNRs

PSR Name	P (s)	\dot{P}	Assoc. SNR	τ_c (yr)	SNR age (kyr)	n	Ref.
J0007+7303	0.316	3.61E-13	CTA1	1.39E+4	13^{+2}_{-8}	...	1
J0205+6449	0.066	1.94E-13	3C58	5.37E+3	$0.830, \leq 7$...	2
J0525-6607	8.047	6.50E-11	N49	1.96E+3	6.6	...	3
B0531+21	0.033	4.23E-13	Crab PWN	1.24E+3	0.957	2.51(1)	4
J0537-6910	0.016	5.18E-14	N157B,EXGAL:LMC	4.93E+3	< 5	-1.5	5
J0538+2817	0.143	3.67E-15	S147	6.18E+5	26-34	...	6
B0540-69	0.050	4.79E-13	0540-693,EXGAL:LMC	1.67E+3	0.76 - 1.66	2.140(9)	7
J0821-4300	0.113	1.20E-15	PUPPIS A	1.49E+6	3.3-6.2	...	8
B0833-45	0.089	1.25E-13	Vela	1.13E+4	9-27	1.7	9
J1016-5857	0.107	8.08E-14	G284.3-1.8	2.1E+4	10	...	10
J1119-6127	0.408	4.02E-12	G292.2-0.5	1.61E+3	4.2-7.1	2.91(5)	11
J1124-5916	0.135	7.53E-13	G292.0+1.8	2.85E+3	2.93-3.05	...	12
J1210-5226	0.424	6.60E-17	G296.5+10.0	1.02E+8	7	...	13
B1338-62	0.193	2.53E-13	G308.8-0.1	1.21E+4	32.5	...	14
J1437-5959	0.062	8.59E-15	G315.9-0.0	1.14E+5	22	...	15
B1509-58	0.151	1.54E-12	G320.4-1.2(MSH 15-52)	1.55E+3	1.9	2.839(1)	16
J1550-5418	2.070	2.32E-11	G327.24-0.13	1.41E+3	
J1632-4818	0.813	6.50E-13	G336.1-0.2	1.98E+4	
J1635-4735	2.595	...	G337.0-0.1	
B1643-43	0.232	1.13E-13	G341.2+0.9	3.25E+4	
B1706-44	0.102	9.30E-14	G343.1-2.3	1.75E+4	5	...	17
J1726-3530	1.110	1.22E-12	G352.2-0.1	1.45E+4	
J1734-3333	1.169	2.28E-12	G354.8-0.8	8.13E+3	...	0.9(2)	18
J1747-2809	0.052	1.56E-13	G0.9+0.1	5.31E+3	1-7	...	19
J1747-2958	0.099	6.13E-14	PWN:G359.23-0.82	2.55E+4	...	<1.3	20
B1757-24	0.125	1.28E-13	G5.4-1.2	1.55E+4	14	-1	21
B1758-23	0.416	1.13E-13	W28	5.83E+4	33-36	...	22
B1800-21	0.134	1.34E-13	G8.7-0.1	1.58E+4	15-28	2	23
J1808-2024	7.556	5.49E-10	G10.0-0.3(W31)	218	
J1809-2332	0.147	3.44E-14	G7.5-1.7	6.76E+4	≤ 15	...	24
J1811-1925	0.065	4.40E-14	G11.2-0.3	2.33E+4	0.96-3.4	...	25
J1813-1749	0.045	1.50E-13	G12.8-0.02	4.6E+3	0.285-2.5	...	26
B1823-13	0.101	7.53E-14	GRS:J1825-137,PWN:G18.0-0.7	2.14E+4	...	2	27
J1833-1034	0.062	2.02E-13	G21.5-0.9	4.85E+3	0.72-1.07	1.857(6)	28
J1841-0456	11.779	4.47E-11	Kes 73	4.18E+3	1.1-1.5	...	29
J1845-0256	6.971	...	G29.6+0.1	1.02E+8	≤ 8	...	30
J1846-0258	0.326	7.08E-12	Kes 75	728	0.9-4.3	2.65(1)	31
J1850-0006	2.191	4.32E-15	G32.45+0.1	8.04E+6	
J1852+0040	0.105	8.68E-18	Kes 79	1.92E+8	3-15	...	32
B1853+01	0.267	2.08E-13	W44	2.03E+4	6-29	...	33
J1907+0602	0.107	8.68E-14	G40.5-0.5?	1.95E+4	20-40	...	34
J1907+0919	5.169	7.78E-11	G42.8+0.6	1.05E+3	
J1930+1852	0.137	7.51E-13	G54.1+0.3	2.89E+3	2.5-3.3	...	35
B1951+32	0.040	5.84E-15	CTB80	1.07E+5	60	...	36
J1957+2831	0.308	3.11E-15	G65.1+0.6	1.57E+6	44-140	...	37

Table 1—Continued

PSR Name	P (s)	\dot{P}	Assoc. SNR	τ_c (yr)	SNR age (kyr)	n	Ref.
J2021+4026	0.265	5.47E-14	G78.2+2.1	7.69E+4	6.6	...	38
J2022+3842	0.024	4.32E-14	G76.9+1.0	8.91E+3	5	...	39
J2229+6114	0.052	7.83E-14	G106.6+2.9	1.05E+4	
J2301+5852	6.980	4.84E-13	CTB109	2.28E+5	7.9-9.7	...	40
B2334+61	0.495	1.93E-13	G114.3+0.3	4.06E+4	7.7	...	41

References. — SNR ages: [1] Abdo et al. (2012); Lin et al. (2010), [2] Kothes (2010); Fesen et al. (2008), [3] Park et al. (2003), [4] Albert et al. (2008), [5] Wang & Gotthelf (1998), [6] Kargaltsev & Pavlov (2008); Kramer et al. (2003), [7] Park et al. (2010); Hwang et al. (2001), [8] Becker et al. (2012); Gotthelf & Halpern (2009a), [9] Kargaltsev & Pavlov (2008); Aschenbach et al. (1995), [10] Ruiz & May (1986); Kargaltsev & Pavlov (2008), [11] Kargaltsev & Pavlov (2008); Kumar et al. (2012), [12] Kargaltsev & Pavlov (2008); Winkler et al. (2009), [13] Gotthelf & Halpern (2008), [14] Caswell et al. (1992), [15] Camilo et al. (2009), [16] Fang & Zhang (2010a), [17] Nicastro et al. (1996), [19] Fang & Zhang (2010a), [21] Caswell et al. (1987), [22] Rho & Borkowski (2002); Velázquez et al. (2002), [23] Finley & Oegelman (1994), [24] Roberts & Brogan (2008), [25] Kargaltsev & Pavlov (2008); Tam & Roberts (2003); Kaspi et al. (2001), [26] Fang & Zhang (2010b); Gotthelf & Halpern (2009b), [28] Bietenholz & Bartel (2008); Kargaltsev & Pavlov (2008), [29] Vink & Kuiper (2006), [30] Gaensler et al. (1999), [31] Kargaltsev & Pavlov (2008); Gotthelf et al. (2000), [32] Giacani et al. (2009); Sun et al. (2004), [33] Kargaltsev & Pavlov (2008); Koo & Heiles (1995), [34] Downes et al. (1980), [35] Kargaltsev & Pavlov (2008); Bocchino et al. (2010), [36] Leahy & Ranasinghe (2012); Kargaltsev & Pavlov (2008), [37] Tian & Leahy (2006), [38] Uchiyama et al. (2002), [39] Marthi et al. (2011), [40] Sasaki et al. (2004), [41] Yar-Uyaniker et al. (2004)

Braking indices: [4] Lyne et al. (1993), [5] Middleditch et al. (2006), [7,16,31] Livingstone et al. (2007), [9,21,23,27] Espinoza (2013), [11] Weltevrede et al. (2011), [18] Espinoza et al. (2011), [20] Hales et al. (2009), [28] Roy et al. (2012)